JOURNAL OF GEOPHYSICAL RESEARCH, VOL. 88, NO. C7, PAGES 4355–4367, MAY 20, 1983

Eddy Kinetic Energy in the North Atlantic From Surface Drifters

PHILIP L. RICHARDSON

Woods Hole Oceanographic Institution, Woods Hole, Massachusetts 02543

One hundred ten satellite-tracked freely drifting buoys measured velocities and trajectories of the near-surface currents in the North Atlantic. Mean velocity values and the velocity variance about the mean were calculated for different regions. A horizontal map of eddy kinetic energy was prepared on a 2° × 2° grid between latitudes 20° and 55°N. Maximum eddy energy (~3000 $cm^2 s^{-2}$) coincides with the high speed Gulf Stream jet where it begins large amplitude meanders near 37°N 67°W. A tongue of high eddy energy coincides with the Stream's path eastward and around the Grand Banks into the Newfoundland Basin where values of 1000 $cm^2 s^{-2}$ are found. A weaker tongue extends eastward across the mid-Atlantic Ridge near 45°N. A second weak extension reaches southeastward from the Stream and crosses the mid-Atlantic Ridge between 30° and 35°N. North and south of the Stream, eddy energy diminishes rapidly reaching an *e* folding at 300 km from the axis. Values of 200 $cm^2 s^{-2}$ were observed in the mid-gyre region and 100 $cm^2 s^{-2}$ in the Eastern North Atlantic and North Equatorial Current. Although the gross distribution of eddy energy is similar to that determined from ship drift measurements, there are significant differences. Eddy energy from drifters amounts to about twice the value measured by ship drift in the Gulf Stream and one half the ship drift values in the mid-gyre. It is suggested that these differences are due to the horizontal averaging of mesoscale motion and the errors in navigation, both of which are problems with the ship drift technique.

INTRODUCTION

The eddy kinetic energy of ocean currents is important to measure and map for several reasons. First, eddy kinetic energy is much larger than the energy of the mean currents and is thought to be dynamically significant in driving the mean in some regions of high eddy energy [*Holland et al.*, 1983]. Second, geographical patterns of eddy kinetic energy give clues to ocean dynamics (maxima and minima of eddy energy help us identify sources and sinks of energy). Third, the geographical distribution of eddy energy is needed to help develop realistic models of ocean circulation [*Schmitz and Holland*, 1982]. Fourth, horizontal eddy mixing is approximately proportional to eddy kinetic energy [*Price*, 1983]. To understand the distribution of ocean tracers, we need to know the geographical variations of eddy mixing.

Despite recent efforts to measure and describe the variability of ocean currents, a good quantitative description of the geography of eddy kinetic energy does not yet exist [*Schmitz et al.*, 1983]. The measurements that do exist have been used to construct a qualitative, but still incomplete, picture. The only available world-wide map of eddy kinetic energy is based on ship drift measurements [*Wyrtki et al.*, 1976]. Although this map was a major step forward in showing the broad distribution of eddy energy in the world ocean, problems with ship drift data lead one to question some quantitative results. Two smaller regions have also been mapped by using Lagrangian drifters. *Molinari et al.* [1980] showed the eddy energy in the Caribbean by using drifting buoys, and *Riser and Rossby* [1983] mapped eddy energy in the southwestern Sargasso Sea by using SOFAR floats. These maps need to be expanded before an ocean-wide distribution of eddy energy is obtained.

Recently, freely drifting buoys, remotely tracked by satellite, have been used in large numbers to measure near-surface currents in the North Atlantic. With the aim of better describing the surface current variability in the North Atlantic, drifting buoy data from many sources have been collected and used to prepare a horizontal map of the eddy kinetic energy distribution. Some of these data have also been combined with the SOFAR float and current meter data and have been used to make a vertical section of eddy kinetic energy through the Gulf Stream and subtropical gyre [*Richardson*, 1983*b*].

Paper number 3C0249.
0148-0227/83/003C-0249$05.00

METHODS

Data from 110 freely drifting buoys was accumulated from several sources (Table 1). These data consist of 55 buoy years and 40,000 individual velocity measurements. They are concentrated in the years 1977–1980 and are nearly evenly spaced seasonally (Figure 1, Table 2). Geographically, the highest data density is in the Gulf Stream region.

Although the majority of buoys were accompanied by a drogue and tether when launched, in most cases the drogue became detached, probably after a few months. (Actual drogue-tether lifetimes are not known.) Thus, a large part of the data was obtained from undrogued buoys and is representative of the upper few meters of the water column where the buoy hull was located. Where geostrophic currents are weak and wind stress strong, local wind-generated flow could then dominate over geostrophic flow. Direct wind influence on buoys is discussed in a later section.

Buoy positions were determined from Doppler-shifted radio signals by means of the RAMS, ARGOS, and EOLE systems carried aboard several different satellites. Typically, two good fixes per day were obtained for each buoy, and the rms error of a fix was estimated to be 1–2 km [*Richardson et al.*, 1979]. These errors cause velocity errors of 5 cm/s over 12 hours. The ARGOS system provided more frequent fixes (four–five per day) and a higher accuracy (0.1–0.2 km). Erroneous data were eliminated by visually checking plots of positions and the speeds calculated between positions and by discarding inconsistent values. Trajectories and velocities along trajectories were then computed by fitting a cubic spline function through the retained positions and by interpolating two values per day equally spaced in time. The final

TABLE 1. Sources of Data

Name	Location	Number of Buoys*
P. L. Richardson	Woods Hole Oceanographic Institution, Woods Hole, Mass.	33
W. J. Gould	Institute of Oceanographic Sciences, Wormley, U.K.	14
R. Weir, K. Mooney, D. G. Mountain	Coast Guard Oceanographic Unit, Washington, D. C.	13
D. O. Cook	Raytheon Ocean Systems Company, Portsmouth, R.I.	10
D. F. Paskausky	Coast Guard R and D Center, Groton, Conn.	9
R. W. Trites	Bedford Institute of Oceanography, Dartmouth, N.S., Canada	8
R. E. Cheney	Naval Oceanographic Office, Washington, D. C.	6
D. V. Hansen	Atlantic Oceanographic and Meteorological Laboratories, Miami, Fla.	5
C. K. Ross	Bedford Institute of Oceanography, Dartmouth, N.S., Canada	5
B. Blumenthal	Naval Oceanographic Office, Bay St. Louis, Miss.	3
J. Bisagni	National Marine Fisheries Service, Narragansett, R.I.	2
A. Leetmaa	Atlantic Oceanographic and Meteorological Laboratories, Miami, Fla.	2
V. Klaus	Centre de Recherches Atmospheriques de Magny-les-Homeaux, Saint Remy Les Chevreuse, France	2
J. Fornshell	Coast Guard Oceanographic Unit, Washington, D. C.	1
P. L. Grose	NOAA Environmental Data Service, Washington, D. C.	1
E. G. Kerut	NOAA Data Buoy Office, Bay St. Louis, Miss.	1
A. D. Kirwan	Texas A&M University, College Station, Texas	1
G. Williams	Clearwater Consultants, Inc., Boston, Mass.	1
Total		110

*A few buoys are listed twice because different people provided separate portions of their trajectories.

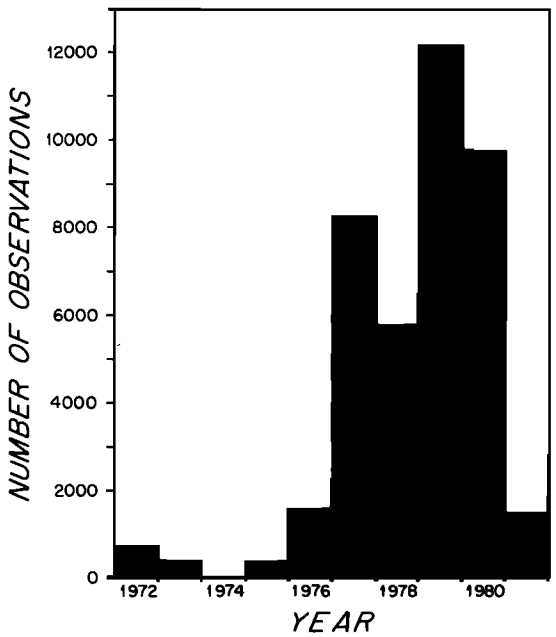

Fig 1*a*. Frequency distribution of the number of semi-daily drifting buoy velocity observations as a function of year.

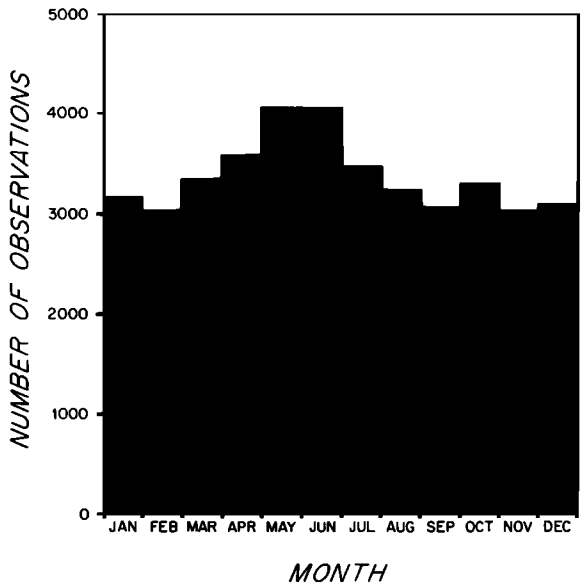

Fig. 1*b*. Frequency distribution of velocity observations as a function of month.

TABLE 2. Summary of the Number of Semi-Daily Observations With Time

	1972	1973	1974	1975	1976	1977	1978	1979	1980	1981	Totals by Month
Jan.		124			62	386	846	495	944	310	3167
Feb.		112			58	336	606	790	897	224	3023
March		106			62	372	645	919	946	292	3342
April		38			127	471	674	1040	1023	220	3593
May					186	620	659	1041	1154	405	4065
June					259	703	459	1330	1302		4053
July				21	251	857	389	1255	681		3454
Aug.				62	186	1021	366	1101	496		3232
Sept.	65			60	89	900	292	1072	584		3062
Oct.	304			62	10	910	303	1001	706		3296
Nov.	200			60	60	818	206	1043	640		3027
Dec.	144			90	236	868	299	1067	406		3110
Total	713	380		355	1586	8262	5744	12154	9779	1451	40424

data set was prepared by smoothing values with a 2.5-day Gaussian-shaped filter to reduce the effect of position errors and to reduce tidal and inertial fluctuations.

The drifting buoys were treated as mobile current meters that gave velocity measurements along their paths. Velocity values were grouped in area and time boxes to give distributions of mean and eddy energy. For each box, the mean velocity $\bar{u}$, $\bar{v}$ in the x and y directions and the departures u', v' from the mean were computed. Eddy kinetic energy values per unit mass were calculated by using $\mathrm{EKE} = 0.5(\overline{u'^2} + \overline{v'^2})$. Velocity variance was calculated for the principal axes [see *Fofonoff*, 1969]. The principal axes are a normal set of coordinates oriented in a direction such that the cross correlation of velocity components vanishes ($\overline{u'v'} = 0$). The basic geographical distributions were made by subdividing the data into 2° × 2° boxes. This size was chosen as being small enough to give the major geographical variation of properties yet large enough to contain sufficient data for statistically significant values. Larger boxes were used to increase the number of degrees of freedom and to characterize larger regions. Since the eddy kinetic energy values are space and time averages, a contribution to eddy energy is given by spatial gradients of velocity within a box. South of Cape Hatteras, the Gulf Stream has relatively small meanders and a large cross-stream velocity gradient; a significant portion of calculated eddy energy in this region is due to the velocity gradient. Downstream from Cape Hatteras, the meander pattern of the Stream is large when compared to its instantaneous width and the contribution from time variability dominates that from velocity gradient.

Over most of the North Atlantic, the eddy energy exceeds the energy of the mean by factors of 2–100. This excess of eddy energy plus the dominant period of the variability, 30–100 days, makes it difficult to resolve accurately the long-term mean without enormous quantities of data. Therefore, the results here are concerned primarily with the variability.

The Lagrangian autocorrelation function has an integral time scale of about 10 days, which is an estimate of the time required for an independent observation of velocity [*Freeland et al.*, 1975; *Price*, 1983]. This implies that 1 degree of freedom is equivalent to the number of semi-daily velocity observations divided by 20 (assuming that individual trajectories are independent).

Many buoys were intentionally launched in Gulf Stream

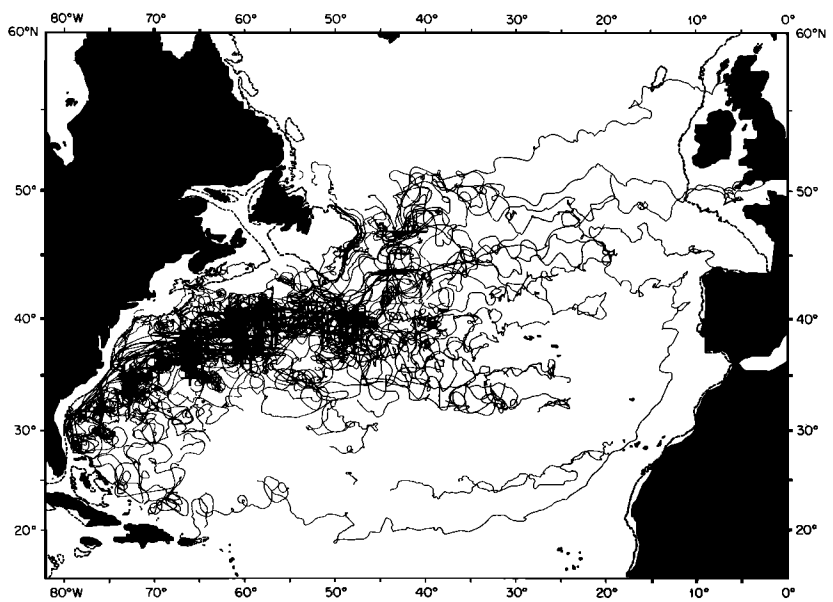

Fig. 2. Summary plot of 110 free drifting buoy trajectories (1971–1981). Buoy data were generously contributed by many individuals (Table 1).

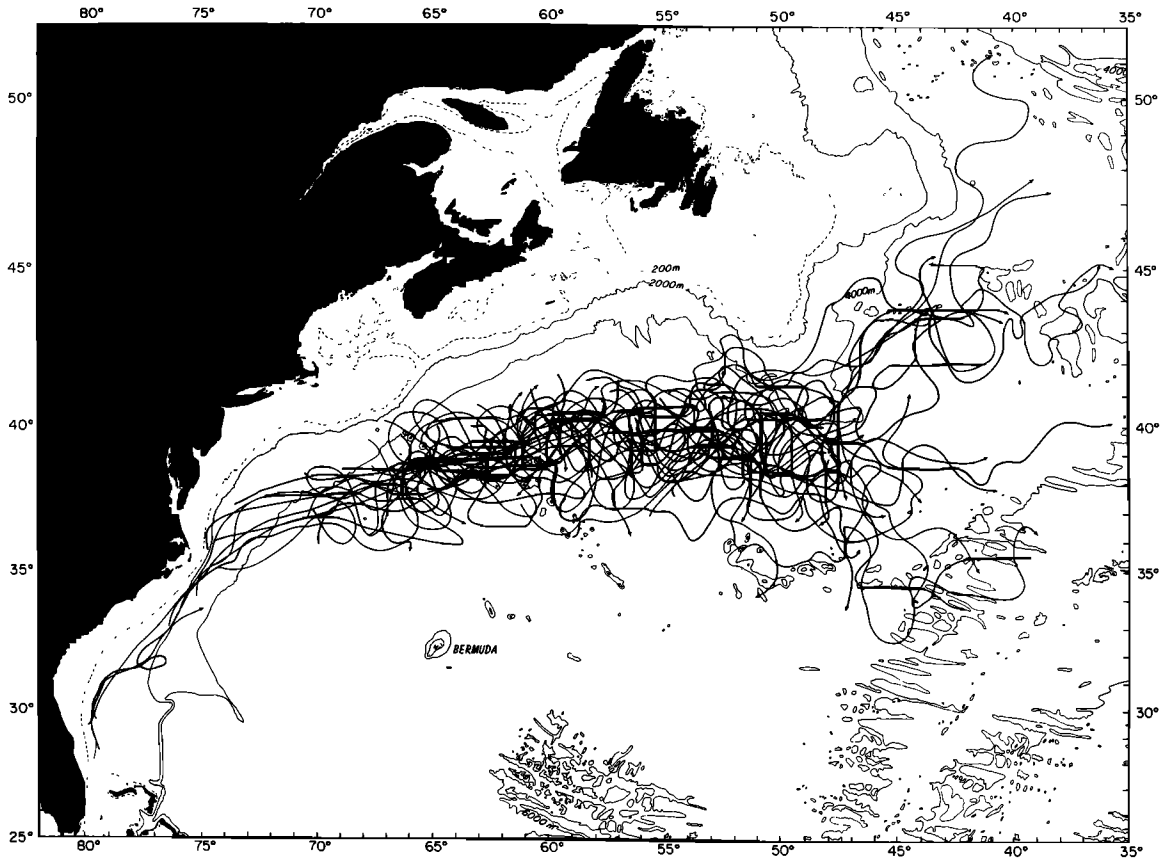

Fig. 3. Gulf Stream trajectories from buoys that moved fast (usually faster than 50 cm s^{-1}) and that did not loop (ring portions were removed). The collection of trajectories shows the beginning of the convoluted meanders east of 70°W, typical envelope of meanders, and divergence of buoys near 40°N 45°W.

rings [*Richardson*, 1980*a*]. Although rings frequently exist near the Stream, using velocities from so many buoys launched in rings would bias the geographical distribution of eddy energy. Therefore, for the 2° × 2° eddy energy map, these ring data were excluded. Data from buoys that entered rings after launch were retained.

RESULTS

Trajectories

Summary plots of the buoy trajectories show well-sampled areas and qualitative features of the flow field (Figure 2). Because the Gulf Stream region is so heavily sampled and

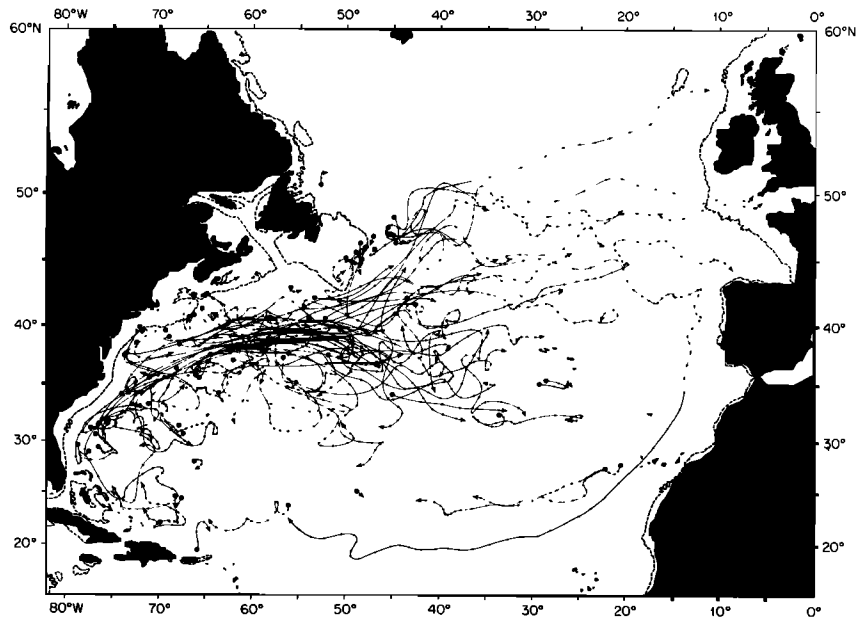

Fig. 4. Buoy trajectories smoothed with a 40-day Gaussian-shaped filter to show large-scale low frequency motion. Large dots mark the beginning of the trajectories, smaller dots are spaced at 15 day intervals.

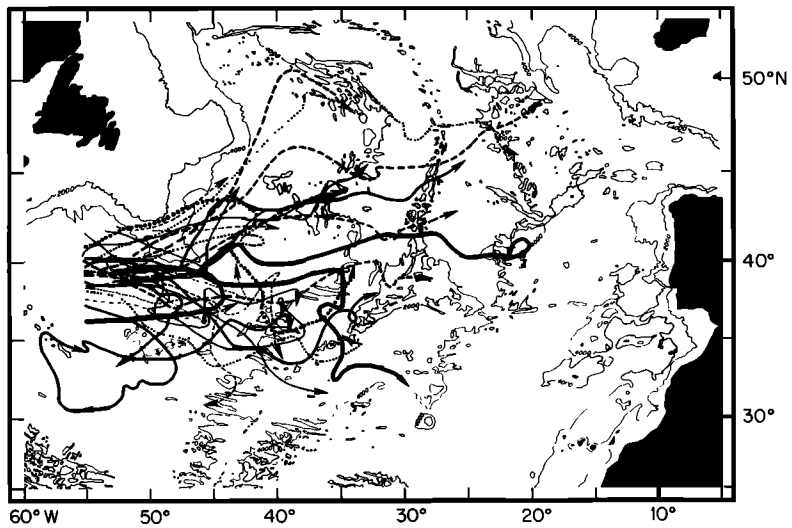

Fig. 5*a*. Smoothed (40*d*) trajectories from buoys originally in the Gulf Stream that drifted eastward past 50°W into the divergence region southeast of the Grand Banks of Newfoundland. Darker lines are not meant to give added importance to trajectories.

populated with rings, a larger scale plot of that region is given (Figure 3) in order to show clearly the character of trajectories there. The high speed Gulf Stream jet is presented by using pieces of individual trajectories selected for the following reasons: (1) the buoys moved rapidly, generally faster than 50 cm/s, and (2) they did not loop (were not in rings) (Figure 3). These trajectories show the increasingly convoluted meanders east of 70°W and the divergence near 40°N 45°W, where the Stream bifurcates into several filaments (or branches). At times, the Stream appears to bifurcate on a synoptic time scale (several buoys rapidly diverge). At other times, the Stream appears to flip-flop in time (several buoys at nearly the same time move south, at another time they move north).

Highly smoothed trajectories reduce the effect of mesoscale eddies and more clearly show the large scale circulation patterns (Figure 4). One drifter launched near the Grand Banks moved eastward toward Spain, southward past the Canary Islands, then westward across the Atlantic. This trajectory is 870 days long and gives an estimate of the circulation time scale of the gyre, which is about 3 years. Gulf Stream buoys arc out toward the area southeast of the Grand Banks near 40°N 45°W where they diverge and decelerate (Figure 5*a*). Yearly summary plots of drifters passing through this region are shown on a larger scale in Figure 5*b*. In general, buoys entering this box north of 39°N went northward, and those that entered south of 39°N went south. Of the 26 buoys that exited the box, 50% went east, 31% went south, and 19% went north. Different years show very different patterns. In 1977, five buoys turned south. Two of these looped over and downstream of the Corner Seamounts [*Richardson*, 1980*b*]. In 1980, six buoys went east, two north, and none south.

The summary trajectory plots (Figures 2–5) display graphically the time-dependent mesoscale fluctuations (seen in trajectories that cross each other) and how these vary geographically. The Gulf Stream is an area of swift currents, large meanders, and intense rings. The regions north and south of the main Stream have a much weaker mean flow, but still strong rings. The Newfoundland Basin also contains high speed current meanders and ring-like eddies, although the speeds are reduced compared to the Stream in the west. In the North Atlantic current region, 40°–50°N, eddy variability decreases toward the east; the mean eastward flow is apparent through the eddies. The North Equatorial Current contains the weakest mesoscale variability of all the areas sampled. Trajectories here are quite smooth in comparison to other areas. In the Antilles Current region, one sees generally slow speeds and large (~200 km diameter) loops in the trajectories. Buoy speeds in the Antilles Current region increase toward the west. South of Bermuda and east of

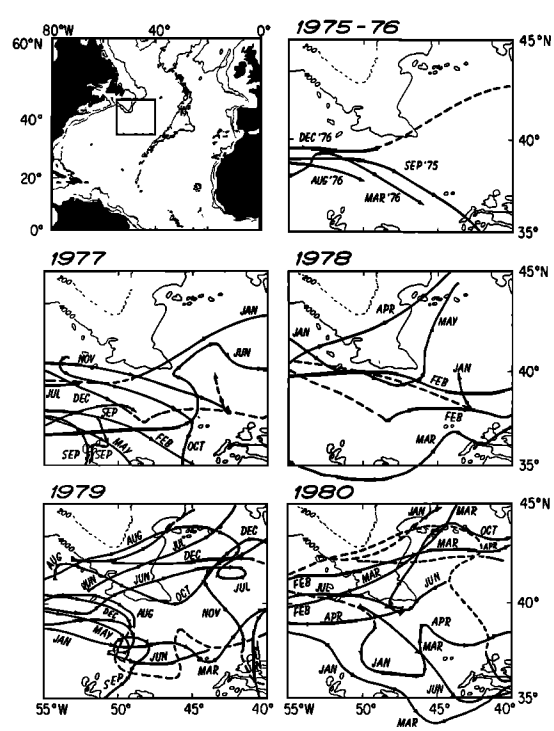

Fig. 5*b*. Yearly summaries of smoothed trajectories of buoys in the Gulf Stream.

TABLE 3. Summary of Average Values in Large Boxes

Location	$\bar{u}$, cm/s	$\bar{v}$, cm/s	MKE, cm²/s²*	EKE, cm²/s²†	EKE/MKE	Number of Observations
Gulf Stream‡				+ 400		
36°–40°N, 58°–70°W	15 ± 6§	2 ± 5	110	1920 − 300	18	3338
Gulf Stream East				+ 430		
38°–42°N, 46°–52°W	18 ± 7	−2 ± 7	170	1280 − 280	7	1513
Newfoundland Basin				+ 210		
45°–52°N, 35°–45°W	8 ± 5	2 ± 4	36	680 − 140	19	1815
North Atlantic Current				+ 60		
40°–50°N, 20°–40°W	9 ± 2	0 ± 2	42	320 − 50	8	3770
North Equatorial Current				+ 40		
18°–30°N, 16°–44°W	−11 ± 2	−3 ± 2	70	110 − 30	2	1415
Antilles Current				+ 80		
20°–26°N, 54°–76°W	−4 ± 3	0 ± 3	7	270 − 60	37	1745
Gyre Interior				+ 90		
28°–31°N, 44°–68°W	4 ± 4	−1 ± 3	10	190 − 50	20	914

*MKE designates mean kinetic energy.
†EKE designates eddy kinetic energy.
‡The Gulf Stream box extends into the region on either side of the Stream where the mean flow is weak and counter to the Stream. Therefore, the mean velocity for this box is much smaller than the central high speed part of the Stream. See Figure 9.
§90% confidence intervals are estimated assuming 1 degree of freedom per 20 semi-daily velocity measurements.

Florida lies the gyre interior where the mean currents are very weak. Here, the eddies, which are also weak, dominate the trajectories. Unfortunately, few trajectories exist in this central gyre region.

The eddy energy values computed for each of these areas demonstrate quantitatively what is observable by simply looking at the trajectories (Table 3, Figure 6). The highest eddy energy is in the Gulf Stream (1920 $cm^2\ s^{-2}$). As we move clockwise around the gyre the eddy energy decreases monotonically to the North Equatorial Current (110 $cm^2\ s^{-2}$). It increases slightly in the interior gyre (190 $cm^2\ s^{-2}$) and Antilles Current (270 $cm^2\ s^{-2}$). The ratio of eddy energy to mean energy gives a quantitative measure of smoothness. The North Equatorial Current, which appears smoothest, has a ratio of 2 as compared with the Antilles Current region, which has a ratio of 37.

Maps on a 2° × 2° Grid

Figure 7 shows the distribution of the number of observations in each 2° × 2° box and Figure 8, the distribution of mean velocity vectors. The map of velocity vectors is noisy because the velocity variance is large when compared with mean. Only much larger numbers of observations (or larger boxes) would give more stable results. The higher mean

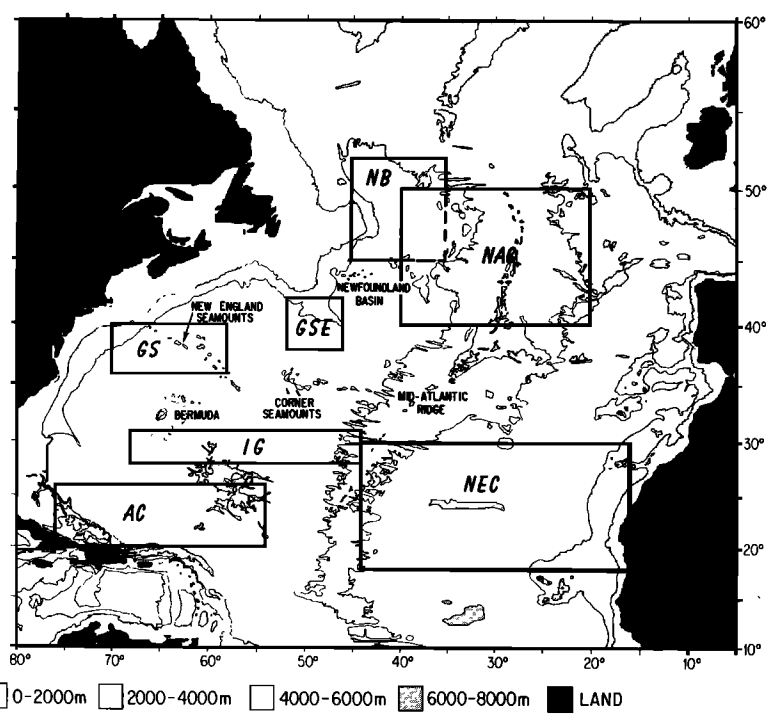

Fig. 6. Location diagram showing large boxes used to calculate summary values given in Table 3.

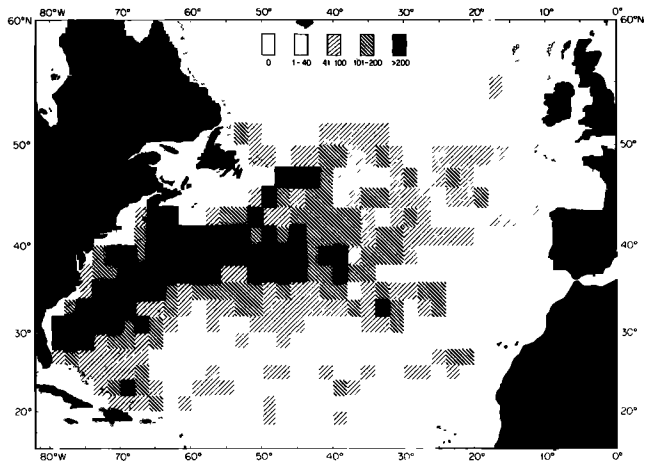

Fig. 7. Map showing the number of semi-daily observations in each 2° × 2° box.

velocity values in the Gulf Stream and North Atlantic Current, and those in other areas where adjacent values agree, are probably correct. Where eddies are strong and the mean weak, the mean vectors are not very reliable.

A velocity profile across the Gulf Stream at 65°W shows a peak mean speed, averaged between 38° and 39°N, of 32 cm s^{-1} and a mean width of about 550 km (Figure 9). A profile at 55°W is similar to this, but shows that the Stream is slightly slower, slightly broader, and centered about 150 km north of its position at 65°W. South of the Stream on both profiles there are negative speeds indicating a countercurrent. However, calculated speeds there are not significantly different from zero at the 90% confidence level.

Values of kinetic energy are stable and show a smooth distribution in space (Figure 10). The distribution is dominated by a sharply peaked ridge of high eddy energy that coincides with the Gulf Stream (Figure 11). Peak values are greater than 2000 cm^2 s^{-2} and reach 3000 cm^2 s^{-2} centered near 37°N 67°W. At this spot, Gulf Stream meanders increase to large amplitude (Figure 3) and rings are often shed. West of this, meanders are usually smaller in amplitude; east of this, speeds in the core of the Stream are lower. This spot also marks the location at which the variance changes from having its major axis directed parallel to the Gulf Stream (and topography) in the west to being more isotropic (Figure 12). Near 55°W the major axis of variance is directed north-south, presumably due to the extremely large amplitude meanders there.

The eddy energy ridge follows the high speed Gulf Stream eastward and around the Grand Banks into the Newfoundland Basin where values of 1000 cm^2 s^{-2} are found. From here, values decrease eastward maintaining a relative high >200 cm^2 s^{-2} across the mid-Atlantic Ridge between 42° and 50°N. A secondary relative high of values up to 500 cm^2 s^{-2} extends southeastward from the bifurcation point near 40°N, 45°W, and crosses the mid-Atlantic Ridge between latitudes 30° and 35°N. Both these eastward extensions of eddy energy are located where mesoscale eddies or current rings have been observed [*Gould*, 1976, 1981; *Emery et al.*, 1980; *Krauss and Meinke*, 1982] and where high eddy potential energy density exists [*Dantzler*, 1977].

South of the Stream, eddy energy decreases toward the gyre interior where values of 200 cm^2 s^{-2} are found (except in the west near the Bahama Islands). The decrease away from the Stream also occurs to the north where the 200 cm^2 s^{-2} contour lies near the continental shelf boundary. Most of the decay in energy from the peak occurs over a short space-scale compared to the gyre. Along 65°W the *e* folding scale is ~300 km (Figure 11).

A bulge of high eddy energy (1000 cm^2 s^{-2}) extends southeastward from the main Stream near 60°W. This feature appears to be associated with the line of New England Seamounts, which the Gulf Stream crosses at that point. Frequently, buoys moving eastward in the Stream were observed to become trapped and to make many loops in a ring-meander which was located over or near the Seamounts [*Richardson*, 1981].

On both sides of the Stream, high eddy energy coincides

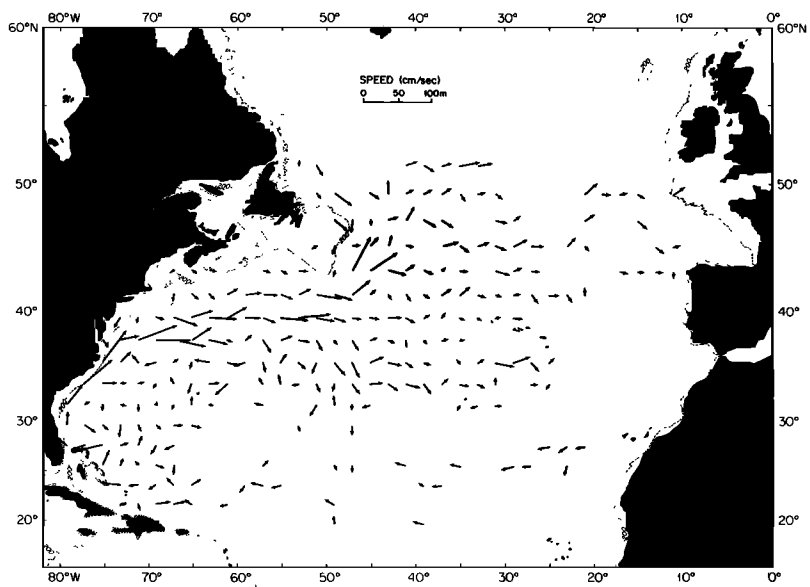

Fig. 8. Mean velocity vectors based on all values in 2° × 2° boxes. Boxes containing fewer than 40 observations were omitted. Tail of arrow is proportional to speed. Values in the Gulf Stream reach 60 cm s^{-1} near 37°N 71°W.

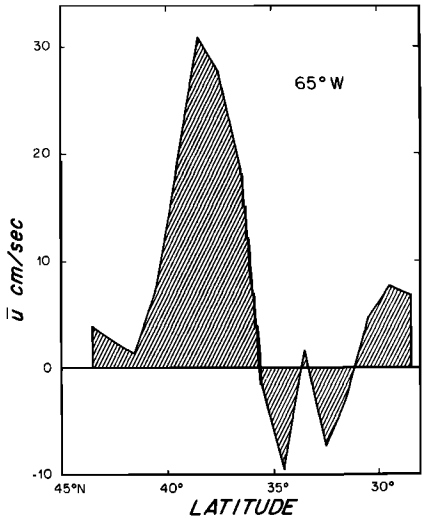

Fig. 9a

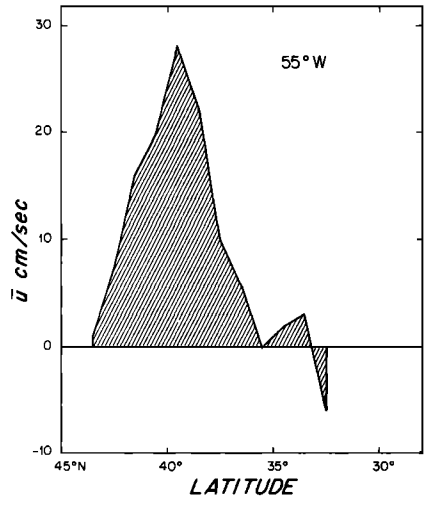

Fig. 9b

Fig. 9. Profiles of eastward velocity across the Gulf Stream at 65°W and 55°W. Values are averages of velocity observations in 1° × 10° boxes, each box containing at least 200 observations. The 90% confidence limits are estimated to be ±5–10 cm s^{-1} at the edges of the Stream at 65°W, ±20 cm s^{-1} at the peak speed at 65°W, and ±10 cm s^{-1} across the profile at 55°W. One degree of freedom was assumed to exist for every 20 semi-daily velocity observations.

with areas in which rings have been observed [*Parker*, 1971; *Lai and Richardson*, 1977; *Richardson*, 1983*a*]. South of the Stream, eddy energy decreases rapidly with decreasing latitude to 30°N, where it becomes nearly constant. The southern boundary of the ring population (except in the west) is also located near 30°N. The effects of including buoys launched in rings and also of smoothing data is shown in Figure 13 (Table 4). Rings broaden the high energy region to the south of the Stream where most rings were observed. Smoothing with a 2.5 day Gaussian-shaped filter decreases eddy energy, especially just south of the Stream's axis where the most energetic rings are found. Many of these rings have a low period of rotation ~2 days. An extreme example, ring Bob, was located near 35°N 69°W and had an associated eddy kinetic energy of 9500 cm^2 s^{-2} before smoothing and 1400 cm^2 s^{-2} afterward; its period of rotation was approximately 2.3 days.

The source of high eddy kinetic energy is clearly the Gulf Stream. However, it is not obvious which of several mechanisms are the most important in causing the observed distribution of eddy energy. The relevant possibilities are thought to be local instability of the Gulf Stream and its recirculation [*Pedlosky*, 1964], energy radiated from these currents [*Talley*, 1982], and rings that can transport and radiate energy as they migrate through the ocean [*Flierl*, 1977, 1981].

We attempted to define a seasonal variation of eddy energy in larger boxes by subdividing data into monthly subsets (Figure 14). While considerable variability exists in monthly values, there is little evidence for an obvious seasonal signal except in the North Atlantic Current and possibly in the Gulf Stream (east) and Interior Gyre. Most monthly variability appears to be noise caused by a decimation of the data and a decrease in the degrees of freedom. In the North Atlantic Current, data were subdivided into three sets, one in 1975–1978 and two in 1979–1980. Eddy energy values were recalculated for bi-monthly periods. All three sets show a similar annual amplitude 90 cm^2 s^{-2} and a mean of 250 cm^2 s^{-2} (Figure 15). This annual signal is presumably caused by seasonal wind-stress forcing in this region [*Leetmaa and Bunker*, 1978; *Bunker and Goldsmith*, 1979]. However, the wind-eddy energy and buoy-eddy energy variations are clearly not in phase (Figure 15), and thus, a direct connection between the two is not obvious. Peak wind-eddy energy occurs in January and February. Peak surface-current eddy energy occurs in May and June, 4 months later. Since a seasonal fluctuation of eddy energy has been observed with current meters in the eastern North Atlantic [*Dickson et al.*, 1982], it is not surprising to see seasonality in the near-surface buoy measurements. However, it should be stressed that the seasonal signal is scarcely above sampling error.

DISCUSSION

The general pattern of variability determined from drifting buoys (Figure 10) is similar to that from ship drift measurements [*Wyrtki et al.*, 1976], although there are significant differences. One difference is that the buoy map shows a maximum in eddy energy with a peak value of 3000 cm^2 s^{-2} located where the Gulf Stream forms large amplitude meanders. (*Kirwan et al.* [1976] report much higher values of kinetic energy in the Stream. The main reasons for this discrepancy are that (1) Kirwan et al. used a single buoy that was embedded in the high velocity part of the Gulf Stream and (2) they calculated kinetic energy along the trajectory, not mean eddy kinetic energy.) The ship drift map shows a gradual decrease in eddy energy eastward from a high of 2000 cm^2 s^{-2} located in the Florida Current off the coast of South Carolina. A second, major difference is that values of eddy energy from buoys are about 2 times higher than ship drift values in the Gulf Stream after it has left the coast but lower by about one half in the low energy interior (Figure 16). This represents a factor-of-4 difference in the two techniques between high and low energy regions.

Peak values in the Gulf Stream near 65°W are ~3000 cm^2 s^{-2} from buoys (Figures 10 and 11) and ~1200 cm^2 s^{-2} from ship drift [*Wyrtki et al.*, 1976, Figure 2], in the gyre interior also near 65°W ~200 cm^2 s^{-2} from buoys (Figure 10, Table

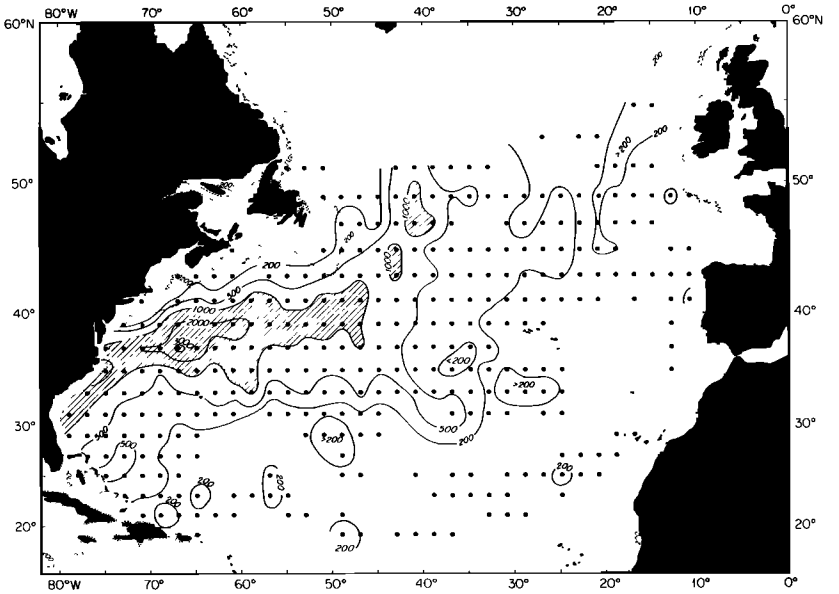

Fig. 10. Eddy kinetic energy ($cm^2\ s^{-2}$) based on values in 2° × 2° boxes. Dots show location of boxes containing greater than 20 observations. A peak in eddy energy of 3000 $cm^2\ s^{-2}$ coincides with the high speed and convoluted meander region of the Gulf Stream. Low values of eddy energy, 100–200 $cm^2\ s^{-2}$, are found in gyre interior, eastern Atlantic, and North Equatorial Current.

3), and ~350 $cm^2\ s^{-2}$ from ship drift [*Wyrtki et al.*, 1976, Figure 2]. The minimas in both distributions are located in the eastern North Atlantic and are ~100 $cm^2\ s^{-2}$ from buoys (Table 3) and ~300 $cm^2\ s^{-2}$ from ship drift [*Wyrtki et al.*, 1976, Figure 4].

The lower ship drift values in the Gulf Stream are probably due to the averaging length (~400 km) of a typical velocity measurement, which is larger than the typical width of the Stream or the diameter of a mesoscale eddy. Thus, ship drift measurements average spatially over much of the mesoscale eddy variability. However, in the low energy interior, ship drift values are higher by a factor of 2. This is probably due to inaccuracies in ship drift velocity determinations. A ship drift determination of a surface current velocity is calculated as the difference between the vector that joins two consecutive position fixes and the mean dead reckoning velocity over the same period of time. Dead reckoning combines estimates of the average course steered and average speed of the ship through the water. These values are uncertain to an estimated (by the author) ±1° in course and ±0.33 knots (17 cm s^{-1}) in speed. Errors of this magnitude, combined with position errors of ±2 km, give errors in current velocity of approximately 20 cm s^{-1}, an apparent eddy energy of approximately 200 $cm^2\ s^{-2}$ (in addition to real eddy energy). Buoy velocity errors, approximately 5 cm s^{-1}, are significantly smaller than this. This apparent eddy energy could account for the difference between eddy energy values calculated form buoy data and those from ship drift data in both the interior gyre and the Eastern North Atlantic. The implication is that the whole distribution of eddy kinetic energy determined from ship drift is inflated by ~200 $cm^2\ s^{-2}$.

The significance of this is that the real eddy energy variations (from buoys) between gyre interior (200 $cm^2\ s^{-2}$) and Gulf Stream maximum (3000 $cm^2\ s^{-2}$) is a factor of 15, not 3.5 as implied by the ship drift map. This variation factor (15) also agrees with *Dantzler*'s [1977] map of eddy potential energy density, where values range from ~100 $cm^2\ s^{-2}$ to greater than 1600 $cm^2\ s^{-2}$, and the general pattern agrees closely with that of Figure 10. The one major discrepancy between buoy eddy energy and Dantzler's eddy potential

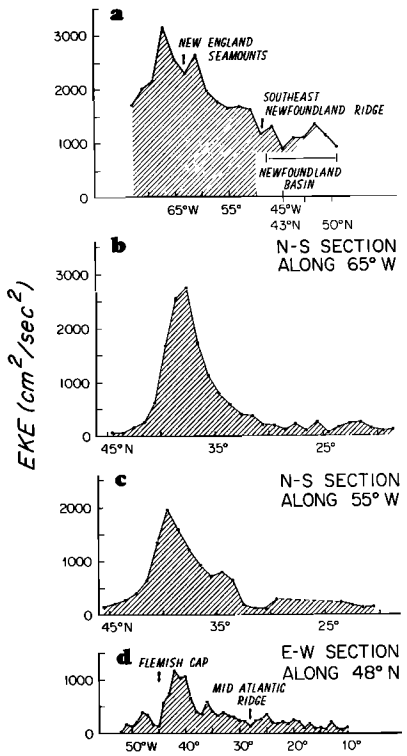

Fig. 11. Profiles of eddy kinetic energy (*a*) along the Gulf Stream axis and into the Newfoundland Basin, (*b*) across the Gulf Stream at 65°W, (*c*) across the Gulf Stream at 55°W, and (*d*) along the North Atlantic Current at 48°N. Values were computed in 2° × 2° boxes along the Gulf Stream; 1° × 10° boxes along 65°W, 55°W, and 48°N.

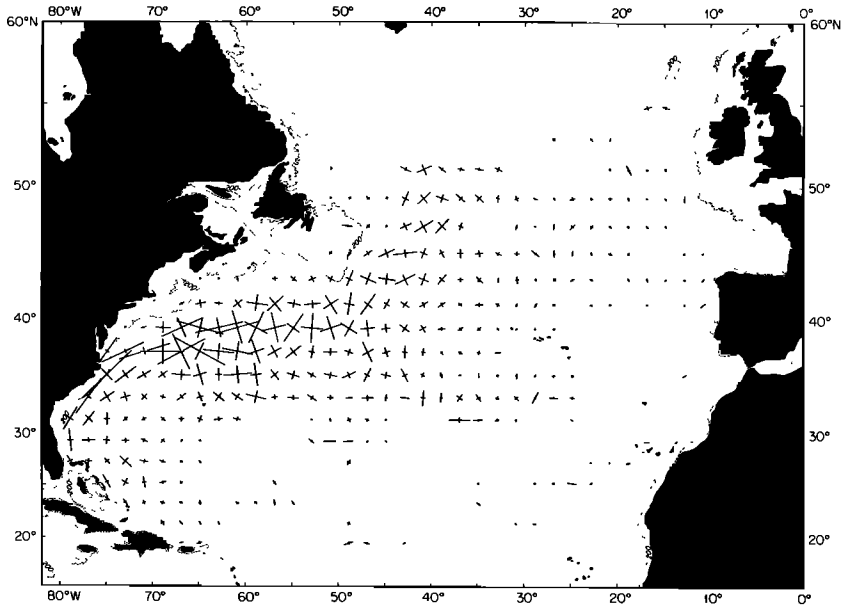

Fig. 12. Principal axes of variance computed in 2° × 2° boxes containing greater than 20 observations. Maximum value in the Gulf Stream near Cape Hatteras 35°N 75°W is 4620 $cm^2\ s^{-2}$.

energy density distribution occurs north of the Gulf Stream where values of potential energy greater than 1600 $cm^2\ s^{-2}$ are found skewed north of the kinetic energy peak (Figure 16*b*). This region of high eddy potential energy is caused by the disappearance of 18° water north of the Stream and is misleading when interpreted as being an average over a constant depth layer. Dantzler calculates eddy potential energy density with the following formula, EPE = $\frac{1}{2}N^2\zeta^2$. N^2 is the depth-averaged value of the squared Brunt-Väisälä frequency from the 18°C isotherm to the 9° isotherm or from the surface temperature to 9° isotherm if the surface temperature was less than 18°C. ζ^2 is the squared rms fluctuation of the 15° isotherm. North of the Gulf Stream, the 18° thermostad disappears, and N^2, which is calculated over a depth range about one half that south of the Gulf Stream, is approximately 3 times larger than the N^2 south of the Stream. Recently, eddy potential energy density has been recalculated by *Emery* [1983] who finds peak values in the Stream of ~3000 $cm^2\ s^{-2}$ and a pattern similar to Figure 10. There is, in addition, good agreement between the eddy kinetic energy distribution and that of mesoscale sea height variability measured by satellite altimetry [*Cheney et al.*, 1983].

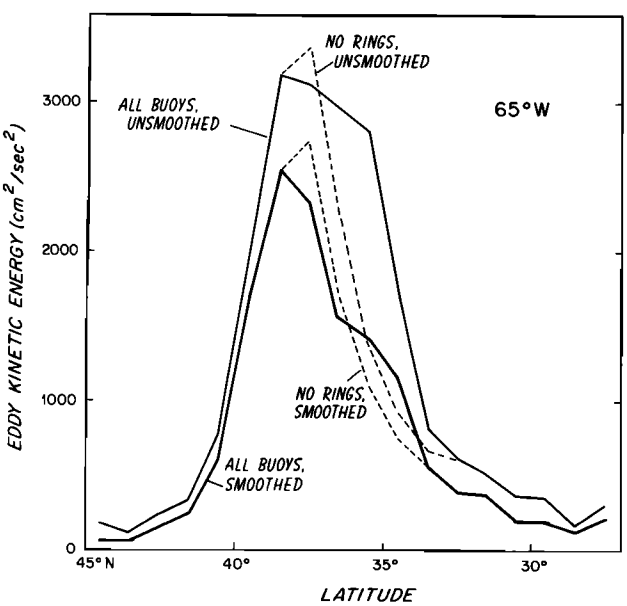

Fig. 13. Eddy kinetic energy calculated in 1° × 10° boxes centered along 65°W. Different curves show the effect of smoothing (2.5 day Gaussian filter) the data and excluding ring observations (buoys launched in rings).

Winds

Two questions concerning the role of the wind need to be answered: First, what is the contribution to trajectories, velocities, and eddy energies of local wind-driven currents as compared with geostrophic currents? Second, to what extent is the buoy measurement of water velocity contaminated by wind or waves pushing the hull through the water? These questions are difficult to answer quantitatively because most buoys in this study were in swift currents and high eddy energy regions where the local wind influence is difficult to detect. In these areas and where XBTs and

TABLE 4. Peak Eddy Kinetic Energy in Gulf Stream

2° × 2° Box at 37°N 67°W	Eddy Energy ($cm^2\ s^{-2}$)	
	Unsmoothed	Smoothed*
All buoys	3740	2200
Rings removed	3910	3150†
Rings only	3170	1140
Ring Bob‡ (35°N 69°W)	9470	1410

*Data smoothed with a 2.5 day Gaussian shaped filter.

†Shifting box center 1°N and 1°W results in slightly different peak values: 2890, 3000, 2850 $cm^2\ s^{-2}$. This shift causes another peak (3220 $cm^2\ s^{-2}$) to emerge near 38°N 64°W.

‡Buoy was looping around the center of ring Bob with a period of 2.3 days.

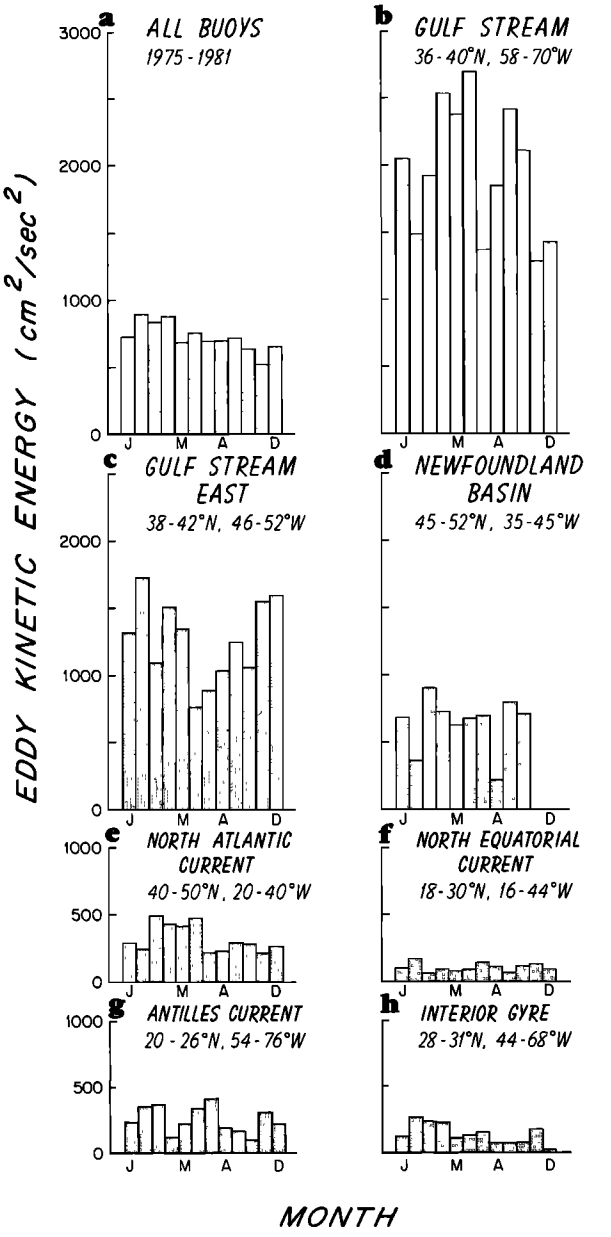

Fig. 14. Monthly values of eddy kinetic energy for seven specific geographical areas (see Figure 6). The North Atlantic Current provides the best evidence of seasonal variation in energy.

hydrographic measurements were available, buoys appeared to follow closely geostrophic currents [*Parker*, 1972; *Richardson*, 1980*b*, 1981; *Gould*, 1981; *Krauss and Meinke*, 1982]. This is most obviously true for buoys, both drogued and undrogued, that swirled around eddies and rings for long periods of time despite strong winds [*Richardson et al.*, 1979; *Richardson*, 1980*a*, *b*]. Further qualitative evidence of buoys measuring geostrophic currents is the close agreement between distributions of buoy kinetic eddy energy and the distribution of eddy potential energy associated with vertical displacements of the thermocline [*Dantzler*, 1977].

It should be easiest to observe local wind-driven currents in regions of low eddy energy and high wind speed variability. Unfortunately, we have few trajectories in these areas. Recently, *Madelain and Kerut* [1978] and *Colin de Verdière* [1983] described measurements of 16 drifters, drogued to a depth of 100 m, in the eastern North Atlantic near 47°N 11°W. The eddy kinetic energy determined from these buoys was 102 $cm^2\ s^{-2}$ [*Colin de Verdière*, 1983]. It was concluded that the wind contamination of buoy motion was of secondary importance to the effect of mesoscale eddies. The energy level of a neutrally buoyant float in the mixed layer was very similar to that of the buoys [*Colin de Verdière*, 1983]. The eddy energy value of 102 $cm^2\ s^{-2}$ from 1250 velocity measurements agrees very closely with a value of 126 $cm^2\ s^{-2}$ calculated here from a different set of 479 observations in the same general vicinity, 44°–51°N, 9°–17°W. Although most of the buoys of *Madelain and Kerut* [1978] remained near their launch location, our drifters in that region had a mean eastward velocity component of 8 cm/s. Despite this discrepancy (which may be due to differences between drogued and undrogued buoys), the agreement in energy values in such a low energy region suggests that the eddy energy distribution (Figure 10) is not dominated by wind variability.

Further information on the influence of winds on buoy velocity comes from numerous drifters in a low eddy energy, high wind region of the eastern North Pacific [*Kirwan et al.*, 1978; *McNally*, 1981]. No difference was seen between drifters drogued with a parachute in the mixed layer at 30 m and drifters with drogues that had become detached [*McNally*, 1981], although there was a difference between buoys with drogues in the mixed layer and those with drogues below the mixed layer. This implies that windage on these buoys even without drogues was not dominant and that the drifters measured the rather uniform (vertically) velocity of the mixed layer. McNally concluded that in windy conditions his drifters, and by inference, the mixed layer currents,

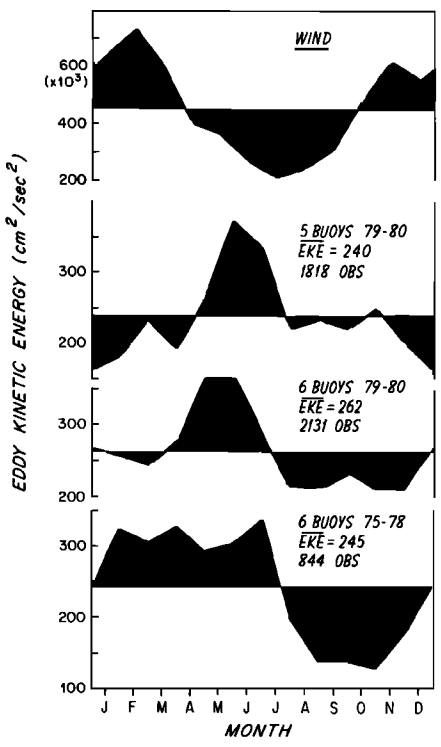

Fig. 15. Annual variation of wind and buoy eddy kinetic energy in the North Atlantic Current region, 40°–54°N 10°–38°W. Monthly wind values are from A. Bunker's compilation available in Woods Hole. Buoy values are calculated from bimonthly periods by using three different groups of buoys.

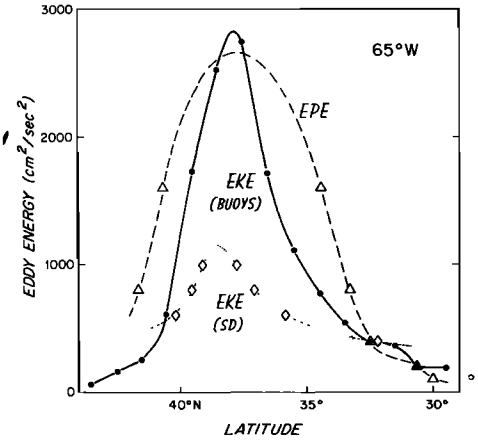

Fig. 16*a*

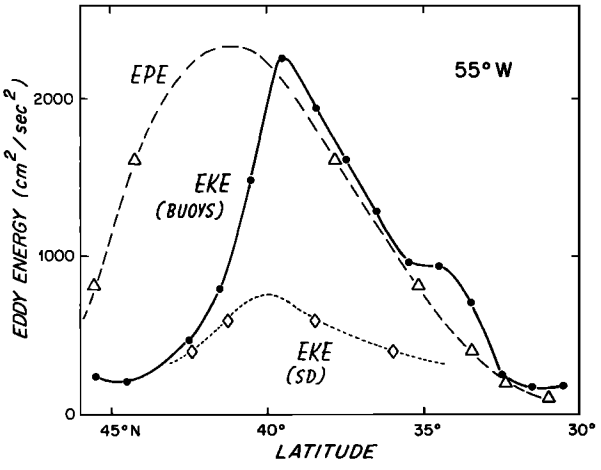

Fig. 16*b*

Fig. 16. Profiles of eddy kinetic energy (EKE) along (*a*) 65°W and (*b*) 55°W from drifting buoys (1° × 10° box averages) and ship drift [*Wyrtki et al.*, 1976, Figure 2] and eddy potential energy (EPE) from vertical displacements of the thermocline [*Dantzler*, 1977, Figure 3]. The maxima in ship drift EKE and EPE are inferred from the trend between contour-latitude values.

systematically moved about 30° to the right of the surface wind at approximately 1.5% of the wind speed. Thus, the Pacific buoy trajectories were strongly influenced by the local wind field during most of the year. If we couple the 1.5% factor with values of wind eddy kinetic energy values for the North Atlantic Current region from Bunker's wind compilations, we arrive at a mean of about 100 cm^2 s^{-2} and a seasonal amplitude of 50 cm^2 s^{-2} as being representative of wind-induced eddy kinetic energy variations of the mixed layer in the North Atlantic Current. The seasonal amplitude is nearly equivalent to the amplitude of seasonal variation in eddy energy in the North Atlantic Current (Figure 15), yet the connection between local wind forcing and current eddy energy in the North Atlantic Current is not direct because the currents lag behind the wind forcing by four months. This lag also implies that buoy slippage (due to winds and waves) is not strongly contaminating the results.

To conclude the discussion of winds, undrogued buoys and those drogued in the mixed layers can be influenced by strong local winds in regions of weak geostrophic currents and low eddy energy. In these areas, winds can generate significant current variability and eddy kinetic energy. However, the magnitude of this wind induced eddy energy (~100 cm^2 s^{-2}) is small when compared with the dominant geographical variations in eddy energy (Figure 10) and, therefore, the eddy energy is not dominated by wind variability. Although monthly eddy energy values do show variability, there is no obvious wintertime peak when wind forcing is strongest. The only area that displays a clear seasonal signal in eddy energy, the North Atlantic Current, has a phase lag of several months between current and wind eddy energy peaks.

Acknowledgments. The research was made possible with funds provided by the National Science Foundation (grant OCE 78-18017). Many people aided the study by generously providing buoy trajectories (see Table 1). T. McKee, R. Goldsmith, and G. Knapp assisted with programing, data processing, and plotting. M. A. Lucas typed the manuscript. W. B. Owens, W. J. Schmitz, J. F. Price, and R. E. Cheney made helpful suggestions. This paper is contribution number 5224 from the Woods Hole Oceanographic Institution.

REFERENCES

Bunker, A. F., and R. A. Goldsmith, Archived time-series of Atlantic Ocean meteorological variables and surface fluxes, *Tech. Rep. WHOI-79-3*, Woods Hole Oceanogr. Inst., Woods Hole, Mass., 1979.

Cheney, R. E., J. G. Marsh, and B. D. Beckley, Global mesoscale variability from collinear tracks of SEASAT altimeter data, *J. Geophys. Res.*, this issue, 1983.

Colin de Verdiere, A., Lagrangian eddy statistics from surface drifters in the eastern North Atlantic, submitted to *J. Mar. Res.*, 1983.

Dantzler, H. L., Potential energy maxima in the tropical and subtropical North Atlantic, *J. Phys. Oceanogr.*, *7*, 512–519, 1977.

Dickson, R. R., W. J. Gould, P. A. Gurbutt, and P. D. Killworth, A seasonal signal in ocean currents to abyssal depths, *Nature*, *295*, 193–198, 1982.

Emery, W. J., Inferred dynamic height, its standard deviation and mesoscale variability in the North Atlantic and North Pacific, *J. Phys. Oceanogr.*, in press, 1983.

Emery, W. J., C. C. Ebbesmeyer, and J. P. Dugan, The fraction of vertical isotherm deflections associated with eddies: An estimate from multiship XBT surveys, *J. Phys. Oceanogr.*, *10*, 885–899, 1980.

Flierl, G. R., The application of linear quasigeostrophic dynamics to Gulf Stream rings, *J. Phys. Oceanogr.*, *7*, 365–379, 1977.

Flierl, G. R., Particle motions in large-amplitude wave fields, *Geophys. Astrophys. Fluid Dyn.*, *18*, 39–74, 1981.

Fofonoff, N. P., Spectral characteristics of internal waves in the ocean, *Deep Sea Res.*, *16* (suppl.), 59–71, 1969.

Freeland, H. F., P. B. Rhines, and H. T. Rossby, Statistical observations of the trajectories of neutrally buoyant floats in the North Atlantic, *J. Mar. Res.*, *33*, 383–404, 1975.

Gould, W. J., A formation zone for Big Babies near the mid Atlantic ridge, *Polymode News*, *16*, October 8, 1976.

Gould, W. J., A front southwest of the Azores, *CM 1981/C:16*, Int. Council for the Explor. of the Sea, Hydrography Committee, 1981.

Holland, W., A Semtner, and D. E. Harrison, Eddy resolving general circulation models, in *Eddies in Marine Science*, edited by A. R. Robinson, Springer-Verlag, New York, 1983.

Kirwan, A. D., Jr., G. McNally, and J. Coehlo, Gulf Stream kinematics inferred from a satellite-tracked drifter, *J. Phys. Oceanogr.*, *6*, 750–755, 1976.

Kirwan, A. D., Jr., G. McNally, E. Reyna, and W. J. Merrell, Jr., The nearsurface circulation of the eastern North Pacific, *J. Phys. Oceanogr.*, *8*, 937–945, 1978.

Krauss, W., and J. Meinke, Drifting buoy trajectories in the North Atlantic Current, *Nature*, *296*, 737–740, 1982.

Lai, D. Y., and P. L. Richardson, Distribution and movement of Gulf Stream rings, *J. Phys. Oceanogr.*, *7*, 670–683, 1977.

Leetmaa, A., and A. F. Bunker, Updated charts of the mean annual windstress, convergences in the Ekman layers, and Sverdrup transport in the North Atlantic, *J. Mar. Res., 36,* 311–322, 1978.

Madelain, F., and E. G. Kerut, Evidence of mesoscale eddies in the Northeast Atlantic from a drifting buoy experiment, *Oceanol. Acta, 1,* 159–168, 1978.

McNally, G. J., Satellite tracked drift buoy observations of the nearsurface flow in the eastern mid-latitude North Pacific, *J. Geophys. Res., 86,* 8022–8030, 1981.

Molinari, R. L., D. K. Atwood, C. Duckett, M. Spillane, and I. Brooks, Surface currents in the Caribbean Sea as deduced from satellite tracked drifting buoys, *Proc. 32 Annual Gulf Carib. Fish. Inst., 32,* 106–113, 1980.

Parker, C. E., Gulf Stream rings in the Sargasso Sea, *Deep Sea Res., 18,* 981–993, 1971.

Parker, C. E., Some direct observations of currents in the Gulf Stream, *Deep Sea Res., 19,* 879–893, 1972.

Pedlosky, J., The stability of currents in the atmosphere and the ocean, 1, *J. Atmos. Sci., 21,* 201–219, 1964.

Price, J. F., Particle dispersion in the western North Atlantic, *J. Geophys. Res.,* in press, 1983.

Richardson, P. L., Gulf Stream ring trajectories, *J. Phys. Oceanogr., 10,* 90–104, 1980*a*.

Richardson, P. L., Anticyclonic eddies generated near the Corner Rise Seamounts, *J. Mar. Res., 38,* 673–686, 1980*b*.

Richardson, P. L., Gulf Stream trajectories measured with free-drifting buoys, *J. Phys. Oceanogr., 11,* 999–1010, 1981.

Richardson, P. L., Gulf Stream rings, in press, in *Eddies in Marine Science,* edited by A. R. Robinson, Springer-Verlag, New York, 1983*a*.

Richardson, P. L., A vertical section of eddy kinetic energy through the Gulf Stream system, *J. Geophys. Res.,* in press, 1983*b*.

Richardson, P. L., C. Maillard, and T. Sanford, The life history of cyclonic Gulf Stream ring Allen, *J. Geophys. Res., 84,* 7727–7741, 1979.

Richardson, P. L., J. J. Wheat, and D. Bennett, Free drifting buoy trajectories in the Gulf Stream system (1975–1978), a data report, *Tech. Rep. WHOI Ref. 79–4,* Woods Hole Oceanogr. Inst., Woods Hole, Mass., 1979.

Riser, S. C., and H. T. Rossby, Quasi-Lagrangian structure and variability of the subtropical western North Atlantic Circulation, *J. Mar. Res.,* in press, 1983.

Schmitz, W. J., Jr., and W. R. Holland, A preliminary comparison of selected numerical eddy-resolving general circulation experiments with observations, *J. Mar. Res., 40,* 75–117, 1982.

Schmitz, W. J., Jr., W. R. Holland, and J. F. Price, Mid-latitude mesoscale variability, *Rev. Geophys. Space Phys.,* in press, 1983.

Talley, L. D., Instabilities and radiation of thin baroclinic jets, Ph.D. thesis, Mass. Inst. of Tech. and Woods Hole Oceanogr. Inst., Cambridge, Mass., June 1982.

Wyrtki, K., L. Magaard, and J. Hager, Eddy energy in the oceans, *J. Geophys. Res., 81,* 2641–2646, 1976.

(Received October 12, 1982;
revised February 7, 1983;
accepted February 7, 1983.)